NISTIR 89-4029

Mixing Motions Produced by Pipe Elbows

T. T. Yeh and G. E. Mattingly

U.S. DEPARTMENT OF COMMERCE
National Institute of Standards and Technology
(Formerly National Bureau of Standards)
National Measurement Laboratory
Center for Chemical Technology
Chemical Process Metrology Division
Gaithersburg, MD 20899

January 1989

NISTIR 89-4029

Mixing Motions Produced by Pipe Elbows

T. T. Yeh and G. E. Mattingly

U.S. DEPARTMENT OF COMMERCE
National Institute of Standards and Technology
(Formerly National Bureau of Standards)
National Measurement Laboratory
Center for Chemical Technology
Chemical Process Metrology Division
Gaithersburg, MD 20899

January 1989

National Bureau of Standards became the National Institute of Standards and Technology on August 23, 1988, when the Omnibus Trade and Competitiveness Act was signed. NIST retains all NBS functions. Its new programs will encourage improved use of technology by U.S. industry.

U.S. DEPARTMENT OF COMMERCE
C. William Verity, Secretary
Ernest Ambler, Acting Undersecretary for Technology

NATIONAL INSTITUTE OF STANDARDS AND TECHNOLOGY
Raymond G. Kammer, Acting Director

MIXING MOTIONS PRODUCED BY PIPE ELBOWS

T. T. Yeh and G.E. Mattingly

Fluid Flow Group

Chemical Process Metrology Division

National Institute of Standards and Technology

Gaithersburg, MD 20899

ABSTRACT

Mixers are critical links in the chain of events and operations that make up a continuous processing system. Mixing can be done using various techniques - stirred tanks, fluid injections schemes, or via a range of elements placed inside pipelines to produce mixedness through the generation of secondary flows and turbulence levels at the expense of fluid pipeline pressure. However, conventional pipeline elements - elbow configurations, reducers, valves, etc. produce pipeflow effects similar to those generated by in-line pipeline mixers. For this reason and for the reason that these elements which, generally, are already in the process piping system - thus adding no additional pressure loss - these elements are examined for their potential as effective pipeline mixers.

Experimental measurements have been made, using laser Doppler velocimetry (LDV) of the pipeflows produced by a range of pipe-elbow configurations. The

secondary flow characteristics of these pipeflows are described qualitatively and quantitatively together with their decay rates in the downstream piping. The potential these flows have as mixing environments is described on the basis of the profiles of the mean and turbulent velocity components, the change of these with downstream distance, and the pressure losses.

Parameters characterizing these flow fields are defined from the measured velocity profiles in a single fluid-water. Conclusions drawn from our results include comparisons of our defined mixing parameters for several elbow combinations. It is concluded that our results should be applicable to pipeflows of miscible fluids having parameters matching those in our study. It is shown that double elbow "out-of-plane" combinations where minimal pipelengths separate the elbows can produce very energetic, long-lasting, swirling flows that can serve as effective mixers. Such effectiveness suggests that process designers might consider adding an additional elbow (and the slight increase in pressure loss) to pipe turns so as to take advantage of the enhanced mixedness that can be achieved via close-coupled elbows-out-of-plane.

INTRODUCTION

Fluid mixing processes are critical to the performance of chemical process productivity. Fluid mixing conditions and fluid or reactant properties, vary widely. To insure effective fluid mixing flow fields are designed to foster interfacial contact so that inter molecular activity can then produce the desired reaction result.

A complete mixing process can be identified by two basic mixing mechanisms: (I) intrinsic physical properties of the mediums, such as the molecular diffusivities which produce micro-scale mixing; and (II) hydrodynamic effects which produce macro-scale mixing. Mixing due to diffusivities is predetermined by the properties of the respective substances and cannot be easily enhanced - given specific pressure and temperature conditions. On the other hand, hydrodynamic mixing is highly dependent on mixer design and is practically the only way to enhance a mixing process.

Hydrodynamic mixer designs are based on the velocity gradients produced in the flow field in the mixer. A process having a uniform velocity field or a region having no velocity gradient would not provide any hydrodynamic mixing. The mixing due to intrinsic molecular diffusivities is normally limited to micro-scale regions. It is very ineffective to mix substances over large spatial scales by just relying on molecular diffusivities. The velocity gradients produced in flow fields in mixers are the main mechanisms to bring separated substances closer and closer together so that the final small scale mixing due to diffusivities can eventually occur. The production of effective velocity gradients is thus used to achieve and maintain phase homogeneity for liquid dispersion, concentration and temperature, etc. and to promote mass/heat transfer in chemical processes.

In general, the hydrodynamics of mixing flows are very complicated. They are combinations of the small scale turbulence and larger scale deformation, entrainment, and swirl. To really understand the mechanisms of flow mixing we would have to study the basic flow field that is used to promote the mixing.

The flow mixing phenomena can be characterized from the velocity field, and this mixing characterization can then be used to identify and evaluate regions of effective or ineffective mixing in specific conditions.

Fluid mixing arrangements include stirred-tank facilities, fluid-fluid injection dynamics, etc. In-line mixers are used to achieve satisfactory mixedness using a wide variety of baffle geometries installed inside pipes that transport fluids between unit operations [1]. These in-line mixers generate interfacial contact surface between fluid species, through turbulence produced by baffle elements, flow parameters, etc. at the expense of static pressure loss. Because of this pressure loss and because of the detrimental aspects of having intrusive baffles inside these pipes - i.e., required cleaning, possible clogging, etc., - other (less costly) mechanisms are considered for generating effective mixing in pipes.

Secondary flows in pipes can be generated in several ways. In straight piping, this can be done via fluid injection effects or asymmetric boundary phenomena or it can be done by pipe elbow effects which is the focus of the present study.

The present study has the objective of evaluating the mixing effectiveness of several selected piping elbow configurations using velocity and pressure measurements. The piping elbow configurations selected are the single, standard, long-radius elbow and several double elbow arrangements produced by these elbows. The double elbow configurations are of the "out-of-plane" type. These arrangements are known, in fluid metering technology,

to be causes of significant metering inaccuracies for meters installed downstream. [2]

The results of the present study will indicate which of these piping configurations should produce the most effective mixing, and the associated pressure losses incurred. The results also give guidance on how an added fluid might be injected into a pipe flow so as to enhance the secondary flow patterns produced by the elbow(s). A central conclusion is that where such pipe line elements as these elbow configurations already exist in chemical processes their capabilities for serving as in-line mixers definitely deserves consideration.

EXPERIMENT

Experiments were conducted in the NIST laser Doppler velocimetry (LDV) equipped Fluid Metering Research Facility. This is a 5 cm (2 in) diameter, D, pipeflow facility which flows water through stainless steel piping. The laser system is described elsewhere,[3]. The source of flow is a NIST fluid metering calibration facility which has a centrifugal pump and a heat exchanger to provide constant temperature flow up to diametral Reynolds number, $W_b D/\nu$, exceeding 10^5 where W_b is the bulk flow velocity and ν is the fluid kinematic viscosity. The thin-walled, round glass pipe that is the test section is contained in a water-filled enclosure having flat, thick (1.9 cm) optical glass sides so that the laser beams are minimally deflected by the curvature of the round glass pipe. This facility can be arranged to place the LDV measurement system approximately 200 pipe diameters downstream from

the exit plane of the elbow configurations. The measurements made include profiles of both streamwise and vertical components of velocity. In this arrangement it is found that the pipeflow is fully developed, and its mean streamwise velocity is described by the appropriate power law distribution.[4] This facility therefore enables characterizations of pipeflow mixing parameters and their decay with downstream distance from a wide range of pipeline elements.

The pipeflows reported here are produced in smooth, stainless steel piping. The joints are arranged through weld-neck type flanges where special attention has been paid to smooth, concentric alignments for all welded joints. All flange joints are concentrically aligned via pins; all flanges are stamped so that re-assembly can be done exactly as done previously. Where steel pipe joins the glass tube test section, extreme care was taken to produce a concentric joint with no steps in the inner pipe diameter.

Four different elbow configurations, three (3) double elbows-out-of-plane and a single elbow, are investigated. Figure 1 shows the sketch of the piping configurations and the coordinate system X,Y and Z with system origin at point O. The radius of the curvature of the elbow is 7.6 cm (3 in). Pressure measurement locations are indicated by A,B,C, and D. Fig.1(a) is for double elbows-out-of-plane configurations which include different spacings, s, and Fig. 1(b) is for the single elbow configuration. In all that follows, coordinates and lengths are non-dimensionalized by the inside pipe diameter, D; all fluid velocities are non-dimensionalized by the bulk flow

velocity in the pipe, W_b. Pressure measurements are specified in terms of "velocity heads" - i.e., $1/2\ \rho\ w_b^2$, where ρ is the fluid density.

RESULTS AND DISCUSSIONS

The characterization of the velocity field is normally given by the random turbulent velocity and the determinable time-averaged velocity. The turbulent field is mainly active over small mixing scales, while the determinable mean velocity field produces large scale entrainment and swirling flows to promote mixedness. In this paper we will report both mean and turbulent velocities, in streamwise and vertical directions, produced by several piping configurations. For the sake of brevity here, results will be presented and discussed mainly for a single flowrate denoted by a diametral Reynolds number, $Re = DW_b/\nu$ of 10^5 and a Dean number, $(Re/2)(D/2r)^{1/2}$ of 28,900, where r is the radius of the curvature of the elbow. The time-averaged velocity components, V and W, respectively, in the streamwise and vertical directions along the horizontal diameter at different axial locations are shown, in figure 2 for both the closely coupled elbows-out-of-plane configuration and the single elbow. In each of these plots, the profiles for the "ideal pipeflows" are the pertinent power law distributions [4] and are denoted by the dotted lines. These distributions would occur after the flow passes through very long lengths of straight, smooth, constant diameter piping.

For the elbows-out-of-plane configuration, the vertical velocity along the horizontal diameter shown in figure 2(a) indicates that this pipeflow has a severe, clock-wise swirl. This severe swirl is distributed along the

horizontal diameter in such a way that there is very little rotation present in the center of the pipe at Z = 2.6. The peaks in the vertical velocity component indicate that very intensive swirl is present in this pipeflow between radial locations $\pm$ 0.2 and the pipe wall. For the ideal pipeflow distribution, the vertical velocity is zero everywhere along the horizontal diameter; this is shown by the dotted line.

As shown in these figures, the streamwise component of this velocity profile at this location is less than the ideal values denoted by the dotted line over most of the horizontal diameter. Over a small interval of the X-axis near X = -0.4 the streamwise velocity exceeds the ideal value. It is clear that this profile is not axisymmetric.

With downstream distance, the vorticity present in this flow diffuses radially inward so as to spin-up the center of this pipeflow. At Z = 31.8, results show that viscous effects have altered the initial profile so that the vertical velocity component indicates that the swirl distribution is essentially that of solid body rotation. At this Z = 31.8 location, the streamwise velocity component shows that it closely approximates that of the ideal profile.

At Z = 91.3, both the vertical and the streamwise velocity profiles approach even more closely that of the ideal profile. However, even at this location the vertical velocity approximates a peak value of 5% of the bulk average velocity.

The single elbow flows at Reynolds number 10^5 are shown in figure 2(b). At the upstream station denoted by Z = 2.7, the vertical velocity component has a peak value that is about 15% of the bulk flow velocity at this Reynolds number. At this location, it is also noted that the streamwise velocity component reaches its peak value of 115% of the bulk velocity. Also at this streamwise location, the vertical velocity component at the pipe centerline is downward at a value of 20% of the bulk velocity while the streamwise component is about 90% of the bulk velocity. The streamwise velocity profile at Z = 2.7 has a slow core that extends over about 60% of the pipe diameter.

At Z = 11.2, the flow from the single elbow has changed significantly and closely approximates that of the ideal profile in about the same way that the flow from the elbows-out-of-plane configuration approximates the ideal flow at Z = 31.8.

Further downstream, at Z = 23.2, the flow from the single elbow has a vertical velocity component that closely approximates zero over the horizontal diameter. The streamwise velocity profile continues to show that the core of this flow is slower than the ideal by about 10% of the bulk velocity. The diameter of this slow core region is about the pipe radius.

Figure 3 presents distributions for the turbulent components of the flow velocity in the vertical and streamwise directions. In each of the graphs shown in figure 3, the fully-developed or "ideal" profiles are denoted by the dotted lines; these ideal profiles were measured by Laufer [5]. The elbows-out-of-plane configuration has peak values for both the vertical and the

streamwise turbulent components near the pipe wall. At the downstream stations Z = 31.8 and Z = 91.3 these distributions change to approximate those of the ideal profiles with peak values found in the flows near the pipe walls.

The flow from the single elbow shown in figure 3(b) has peak values in both the vertical and streamwise turbulent velocity components that occur at different locations from those of the elbow-out-of-plane configuration. The peaks for the single elbow flow occur away from the pipe wall - at radial location of about $\pm$ 0.15% of the pipe diameter for the vertical component and at about $\pm$ 0.30% of the pipe diameter for the streamwise component of the turbulent velocity. With downstream distance, this changes and by Z = 11.2 the peak values in both of these profiles are found near the pipe wall.

From the mean velocity fields, further examination of selected components of the velocity gradient tensor can be done. For convenience, a tensor can be divided into two simpler tensors: a symmetric tensor and an antisymmetric tensor. The symmetric tensor is normally called the deformation tensor and the antisymmetric tensor is related to the flow vorticity, flow swirl or rotation. In general, the deformation tensor contains nine (9) non-zero elements and the swirl tensor contains three (3) elements. However, depending on the geometry of the mixing flow, some elements may be more important than the others. Nevertheless, mixing flows are combinations of turbulence, swirl and deformation both in shear and in stretching. It can be generalized that the larger the deformation or swirl that is present, the better will be the mixing environment.

The concept of material surfaces and deformations due to velocity gradients has been studied very extensively in recent years [6]. It has been shown that material deformation and surface renewal are strongly related to hydrodynamic mixing characteristics. Normally, an increase in material interfacial area or an increase in material deformation implies an increase in the mass transfer or flow mixing. The characterizations of the fluid deformation or the surface stretching are thus one of the more useful parameters for characterizing the flow mixing.

The use of swirl in mixing process is also not new [7,8]. Swirl-circulating, fluidized beds have been used commonly in coal combustors. To increase mass transfer rates, some design modifications - such as helical rather than straight parallel tube arrangements - have been made to produce or enhance secondary flow patterns which will foster swirl and fluid deformation. These secondary flows and the increased turbulent intensity produced by pipe elbows change the pipe flow characteristics and enhance the mixing phenomena in the pipe. These secondary flows also contribute to larger scale mixing by transporting substances from one region to the other; while the increased turbulent intensity accelerates the smaller scale mixing. Based on the measured velocities produced by different piping configurations, several important flow field parameters have been defined and quantified.

These flow field parameters can either characterize the local properties or the average global properties. Besides the turbulent intensity shown early, other local parameters can be defined, based upon the measurements made:

(1) Local swirl intensity: Si = W V X. It is a measure of local angular momentum flux.

(2) Local swirl angle: ϕ = arctan (V/W). It is a measure of the degree of flow relative to the stream direction.

Figure 4 presents, for both piping configurations, the local swirl intensity, and the swirl angle. These parameters are produced using the data shown in figure 2. Figure 4(a) for the elbows-out-of-plane configuration shows swirl intensity distributions which are negative and swirl angles which attain extreme values near the pipe wall. At Z = 2.6, the negative peaks in Si approximately align with the peaks of the mean vertical velocity distributions. That these distributions do not precisely align is due to the product definition of Si. The swirl angle, on the other hand, more closely aligns with the mean vertical velocity component.

Figure 4(b) presents corresponding results for the single elbow flow. It is noted that, again, the swirl angle distribution more closely approximates the mean vertical velocity distribution. The swirl intensity, however, shows a very different character compared to that for the closely coupled elbows-out-of-plane configuration. Near the exit from the single elbow, the swirl intensity changes sign at the pipe centerline and at two other points about the half radius locations along the X axis. At the downstream location, Z = 11.2 this quantitative feature continues to appear, but at X = 23.2, the distribution seems to be monoatonic through the central region of the pipeflow.

As expected, these local parameters which can be considered mixing indices are not uniformly distributed along this pipe diameter. This indicates that some regions are more actively mixed than others. For the double-elbows-out-of-plane configuration, the local swirl intensity is fairly intense and the swirl angle approximates 20 degrees near the pipe wall at the upstream location. The data also indicate that the active mixing regions between these two elbow configurations are quite different. For the double-elbow piping, the most active mixing region is near the wall and there is little mixing activity at the pipe centerline. As for the single elbow case, mixing at pipe centerline is also important. This is because there is only one large swirl eddy produced in the double elbow case and two counter - rotating swirl eddies produced in the single elbow piping. An early conclusion is drawn here that, while there are good mixing regions near the wall for both cases and the pipe centerline for the single elbow, the mixing near the pipe centerline is not very good for the double elbows-out-of-plane configuration. Also as expected, the intensities both for Si and swirl angle decay with downstream distance from both the elbow configurations.

To characterize mixing decay rates, some global parameters are defined and presented. These decays along the pipe downstream of the elbows can be considered to quantify the decay of the global mixing effectiveness in these pipeflows.

(3) Averaged swirl angle:

$Sa = (\phi_{max} - \phi_{min})/2,$

where ϕ_{max} and ϕ_{min} are, respectively, the maximum and minimum local swirl angles at a given axial location Z.

(4) Pipe swirl number:

$$Sp = \int_{-0.5}^{0.5} | Si | dX.$$

An integral of the strength of the local swirl across the horizontal pipe diameter.

(5) Radial shear deformation number:

$$D_{21} = \int_{-0.5}^{0.5} | W \, \partial V/\partial X | d X.$$

An integral of the magnitude of the radial shear deformation, which is one of the nine (9) deformation elements. The streamwise velocity component W is included in the integrand to account for the local mass flux.

(6) Centerline turbulent intensity:

$To = [(v')^2 + (w')^2]^{1/2},$

the root mean-square of turbulent velocity at pipe centerline.

(7) Averaged turbulent intensity:

$Ta = \{ \int_{-0.5}^{0.5} [(v')^2 + (w')^2] dX \}^{1/2}$, the root of the mean-square of turbulent velocity averaged across the horizontal pipe diameter.

Figures 5-7 show the streamwise distributions of these global parameters, Sa, Sp, D_{21}, To, and Ta for three double elbows-out-of-plane configurations with (1) closely coupled, (2) spaced 2.4 diameters and (3) spaced 5.3 diameters and the single elbow configuration.

As shown in figure 5, the averaged swirl angle Sa for closely coupled (S=0) double elbows-out-of-plane is the largest and shows very slow decay with downstream distance. The values of Sa for spaced (s = 2.4 and 5.3 diameters) double elbows-out-of-plane are much smaller than those of the closely coupled case. For the single elbow case, Sa is also, initially, very large but decays very rapidly with downstream distance. These indicate that (1) the closely coupled double-elbows-out-of-plane piping produces very energetic, long-lasting, mixing flows; (2) the spaced (s = 2.4 and 5.3) double-elbows-out-of-plane produce less effective mixing, and; (3) the single elbow produces energetic mixing which is not as long lasting in the downstream pipeflow as in the closely coupled double elbow case.

Figure 6 shows the streamwise distributions of the pipe swirl number Sp, and deformation number D_{21} for all four elbow configurations. Similar to the swirl angle parameter Sa, the closely coupled double-elbows-out-of-plane produces large and long lasting values for Sp and D_{21}. The single elbow, on the other hand, produces large but rapidly decaying values for Sp and D_{21}. The spaced double elbow configurations produce much smaller values of Sp and D_{21}. These results again confirm that the closely coupled double elbows-out-of-plane configuration provides an energetic and long -lasting mixing flow.

The single elbow produces intense mixing, initially, but this decays rapidly with downstream distance. The spaced double elbow configurations provides the least effective mixing flow. It should also be noted that the early conclusion drawn above is based upon these pipeflow conditions; actual mixing efficiency would depend on the initial material conditions or the fluid injection features such as location, velocity, direction, etc. Nevertheless, these flow parameters should be very useful for studying or designing pipeflows to serve as effective mixing environments.

Figure 7 shows the streamwise distributions of the centerline turbulence, To, and the averaged turbulence along horizontal diameters, Ta - for all four elbow configurations. The fully developed pipe turbulence based on Laufer's data are also shown for reference. For all these cases, the initial turbulence levels are all significantly higher than those expected in the fully developed turbulent flows. However, these turbulence levels all decay with downstream distance, Z. Also, there are found relatively small differences in these turbulence quantities for the different piping configurations.

When exponential decay formulas of the form:

$$F = a + b * \exp (- c Z)$$

are fitted to the data for each parameter using the least square error method, the above-described phenomena can be quantified. The initial value b and the decay rates c are useful constants for comparing different piping configurations. Table 1 shows the parameters a, b, and c for the global parameters Sa, Sp, D_{21}, To, and Ta for: (I) closely coupled double elbows-out-

of-plane, (II) 2.4 diameter spaced double elbows-out-of-plane and (III) single elbow. Closely coupled double elbows-out-of-plane ,(I) and single elbow (III) both produced large values for b while the spaced double elbows gave a smaller value for b. Both double-elbows configurations (I) and (II) produced smaller decay rates c, while a single elbow piping ,(III) gave larger values of c.

PRESSURE MEASUREMENTS

Figure 8 shows the sketches of azimuthal locations (looking upstream) of pressure taps at lettered streamwise stations: (a) station A of double elbows-out-of-plane, (b) station A of single elbow and (c) all downstream stations, B, C, and D. Angle values are measured from 12 o'clock clockwise: $\theta_1 = 67.5°$; $\theta_2 = 157.5°$; $\theta_3 = 247.5°$; $\theta_4 = 337.5°$.

Table 2 shows the streamwise station locations, A, B, C and D in diameters, k relative to the system origin for three elbow configurations: (I) closely coupled double elbows-out-of-plane, (II) double elbows-out-of-plane with 2.4 diameter spacing and (III) single elbow. Distances are measured from the system origin along pipe centerline.

Figure 9 presents results for the azimuthal distributions of static pressure in velocity heads, $1/2\ \rho W_b^2$ both upstream and downstream of the respective piping configurations for diametral Reynolds number 10^5. Figure 9(a) shows results for the closely coupled elbows-out-of-plane configuration; the single elbow results are given in figure 9(b). These results indicate, quantitatively, the asymmetry of the static pressure distribution into and out

of these piping configurations. These results also show that the effects of the piping configuration propagate upstream past the inlet to the configuration. For example, the azimuthal distribution denoted by k = -6 shows that, for the closely coupled double elbow configuration, the static pressure at tap No. 4 is higher than that at any other tap. This could be due to the fact that the secondary flow introduced by the first elbow transmits its centrifugal effects on the static pressure at the outside of this elbow. Just downstream from the exit of this configuration, the azimuthal distributions of static pressure are found to be more uniform around the pipe periphery. The interpretation here could be that the single eddy swirl pattern exiting this configuration produces similar centrifugal effects on all these taps. The results shown in figure 9(b) can, for the azimuthal pressure distribution upstream of the single elbow, be interpreted analogously to those for the double elbows. The differences found in the static pressure of the flow entering the single elbow is more uniform than that for the double elbow configuration. The exiting pipeflow indicates that the static pressure at the bottom of the pipe is less than that at the top. To further describe their pressure effects in these pipeflows, we shall use the averaged results from all four taps at each stream station.

Figure 10 shows pressure loss in terms of equivalent smooth straight pipe lengths in diameters versus diametral Reynolds number for three piping configurations. The closely coupled and the spaced double elbow configurations can be compared to conclude that the difference is about five (5) equivalent diameters separating these two results. That the actual difference in pipe length is 2.4 diameters shows that the effect of this swirl

produces essentially a doubling of the pressure loss through the configuration: It is noted that the pressure drop characteristic for these elbows does not change markedly over this Reynolds number range. The single elbow pressure loss characteristic shows a marked change in pressure loss over the diametral Reynolds number range 0-80,000. These pressure losses are noted to increase to essentially match those for the double elbow configuration; these losses are probably associated with the Reynolds number range spanned. It is concluded that this marked increase is due to the double eddy swirl pattern generated in this single elbow and/or flow separation.

The friction factor distributions, $f = \Delta P/(1/2\ \rho W_b^2\ \Delta k)$, versus diametral Reynolds number for different segments of the piping for both the closely coupled double elbow and the single elbow configurations are shown in figure 11. The quantity Δk is the pipelength in diameters over which the pressure change is ΔP. For each piping configuration, the friction factor through the elbow arrangement is significantly larger than in the straight piping downstream of the configuration. The results for the single elbow indicate that the friction factor for pipe segments BC and CD are essentially the same for this range of diametral Reynolds number. This is undoubtedly due to the fact that the secondary flow generated by the single elbow has decayed significantly over the first ten diameters of downstream pipe length. The double elbow results, on the other hand, indicate higher friction factors for segment BC compared to CD, because in these segments the secondary flows have not decayed and therefore produce different effects for friction factor.

Figure 12 presents results for pressure differences in velocity heads

(referenced to the pressure at k = 0.2) for diametral Reynolds number of 10^5 versus streamwise distance, in diameters. Also shown is the distribution for smooth piping. These results show that, for k > 0 the pressure levels in our downstream piping are less than that for smooth pipe. Roughness measurements in our stainless steel piping indicate that our roughness is nominally 125 μ inches; this produces a relative roughness of 6×10^{-5} (normalized by inner pipe diameter). The closely coupled, double elbow configuration is found to have the lowest pressure levels of the three configurations over the streamwise segment k < 80. It is expected that with increased streamwise distance the slopes of these traces would converge to that for the smooth pipe.

SUMMARY AND CONCLUSIONS

In summary, we have, with a limited set of measurements of fluid velocity and pressure, quantified the pipeflows downstream of a standard, single elbow and from several double elbow out-of-plane configurations with different lengths of pipe between the elbows. These pipeflows are found to have different secondary flow characteristics that can serve as in-line fluid mixers and, since these pipeline elements are generally present in the piping systems that are used in the continuous process industry, they do not add to system pressure loss. Of course, where significant fluid injections to pipeflows occur, the measurements made in the present study can be expected to change accordingly. An additional advantage of pipe elbow mixing is that no intrusive elements such as baffles are involved which would increase pressure loss and possible lead to clogging or to increased maintenance requirements.

The present study also includes the definitions of several mixing parameters. These definitions have been tailored to measurements of the velocity profiles. When these parameters are considered locally in these flows, they can indicate regions of high (or low) mixing. When these parameters are integrated, they can be considered globally. These global parameters can then be used: (a) to compare the mixing features of different pipe flows, or (b) to quantify the decay, with downstream distance, of the mixing features of a particular pipe flow.

In conclusion the results of these experiments indicate that these pipe flows can serve as pipe line mixers. These results can be used to specify, according to the presented definitions of fluid mixing parameters, the relative feasibility of using these pipe flows as in-line mixers. These parameters enable comparisons of the different pipeflows. The double elbow-out-of-plane configuration produced a secondary flow that persists over long lengths of downstream piping - especially when the two elbows are closely coupled. However, where it may be desirable to produce short-term mixing, the double eddy secondary motions produced by the single elbow may be more useful.

It is also concluded that the results of these experiments give guidance on how and where fluid injections into these pipe flows might be done. The results of the pressure measurements quantify the loss characteristics of these pipe flows. These are, of course, larger than those found in straight pipe, but they are probably less than those produced by in-line mixers having baffles or other elements intruding into the pipeflow.

It is also concluded that the results of the present study should be corroborated using actual mixing tests where different fluid species are used to assess the mixedness. In this manner, the specific fluid and flow characteristics can be properly arranged to determine the mixing effectiveness of a particular situation.

ACKNOWLEDGEMENT

The authors acknowledge the partial support of the industry-government consortium formed at NIST to investigate pipeflows. The authors also gratefully acknowledge a range of ideas, inputs, and encouragements from the members of this consortium - especially Mr. C. Langford, Mr. T. Miller, and Dr. A. Etchells, who are involved in the chemical industry. Specific thanks also go to Dr. J. Gray, Dr. G. Tatterson and Prof. R. Calabrese for their suggestions and encouragements. The authors gratefully acknowledge the fine secretarial capabilities provided by Mrs. G. Kline. Without these and the patience applied with these capabilities, this paper would not be where it is.

REFERENCES

1. Gray, J. B. "Turbulent Radial Mixing in Pipes" in Mixing, Theory and Practice, Vol. III, Edited by Uhl and Gray, 1986 Academic press.
2. Mattingly, G.E. and Yeh, T.T., "Flowmeter Installation Effects" Procs National Conference of Standards Laboratories Annual Conference, Wash., DC, Aug. 14-18, 1988, published by NCSL, Boulder, CO.
3. Yeh, T.T., Robertson, B., and Mattar, W.M., "LDV Measurements Near a Vortex Shedding Strut Mounted in a Pipe," Journal of Fluids Engineering, ASME Vol. 105, pp.185-196, June 1983.
4. Schlichting, H., Boundary Layer Theory, McGraw-Hill Co., New York, 1968.
5. Hinze, J.O., Turbulence, McGraw-Hill Co., New York, 1959 (Laufers data in Chapter 7).
6. Ottino, J.M., Ranz, W.E., and Macosko, C.W., "A Framework for Description of Mechanical Mixing of Fluids", AIChE J. Vol.27, no.4, p.565, July 1981
7. Lilley, D.G. "Prediction of Inert Turbulent Swirl Flows", AIAA J., Vol 11, no.7, p.955, July 1973
8. Smith, P. J., Smoot, L.D., and Hill, S.C. "Effects of Swirling Flow on Nitrogen Oxide Concentration in Pulverized Coal Combustors", AIChE J., Vol. 32, No.11, Nov. 1986, p.1917

Table 1 Decay Parameters For Sa, Sp, D_{21}, To, and Ta

$$F = a + b \cdot \exp(-cz)$$

F	Parameters			Elbow Configuration
	a	b	c	
Sa (Deg)	0	15.5	0.026	I
	0	2.93	0.026	II
	0	20.0	0.188	III
Sp	0	0.33	0.022	I
	0	0.007	0.023	II
	0	0.033	0.135	III
D_{21}	0	0.559	0.024	I
	0	0.236	0.049	II
	0	1.025	0.148	III
To	0.049	0.075	0.017	I
	0.049	0.095	0.048	II
	0.049	0.137	0.081	III
Ta	0.074	0.060	0.022	I
	0.074	0.048	0.022	II
	0.074	0.121	0.114	III

Double Elbows-Out-of-Plane:

Closely Coupled, (I)
Spaced 2.4 Diameters, (II)

Single Elbow, (III)

Table 2 - Streamwise Station Locations in Diameters (k) Relative to the Origin. Distances are Measured Along Pipe Centerline.

Elbow Configurations	Axial location, k			
	A	B	C	D
I	- 6.0	1.4	25.1	72.1
II	- 8.4	1.4	25.1	72.1
III	- 3.7	1.4	13.4	37.1

Double Elbows-Out-of-Plane:

Closely Coupled, (I)
Spaced 2.4 Diameters, (II)

Single Elbow, (III)

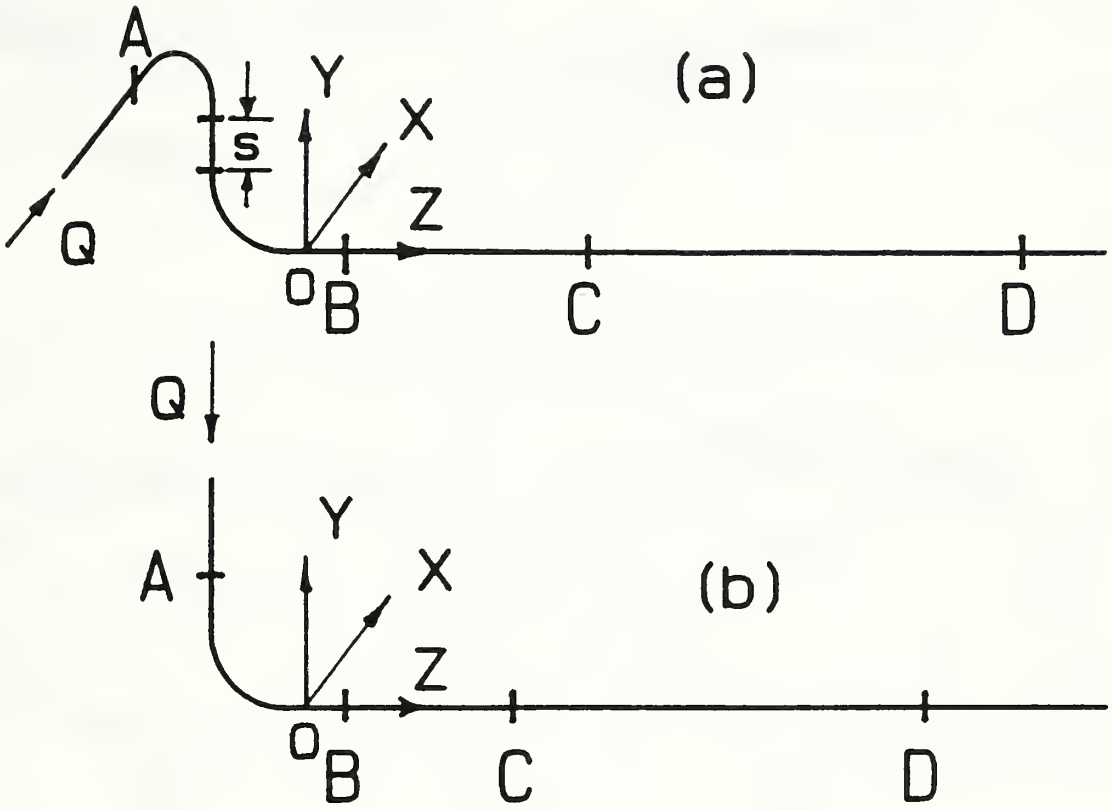

Figure 1 - Sketch of Piping Configurations, Coordinate Systems (origin at 0), and Pressure Measurement Locations: A,B,C, and D: (a) Double Elbows-Out-of-Plane (Different Spacings, s), and (b) Single Elbow.

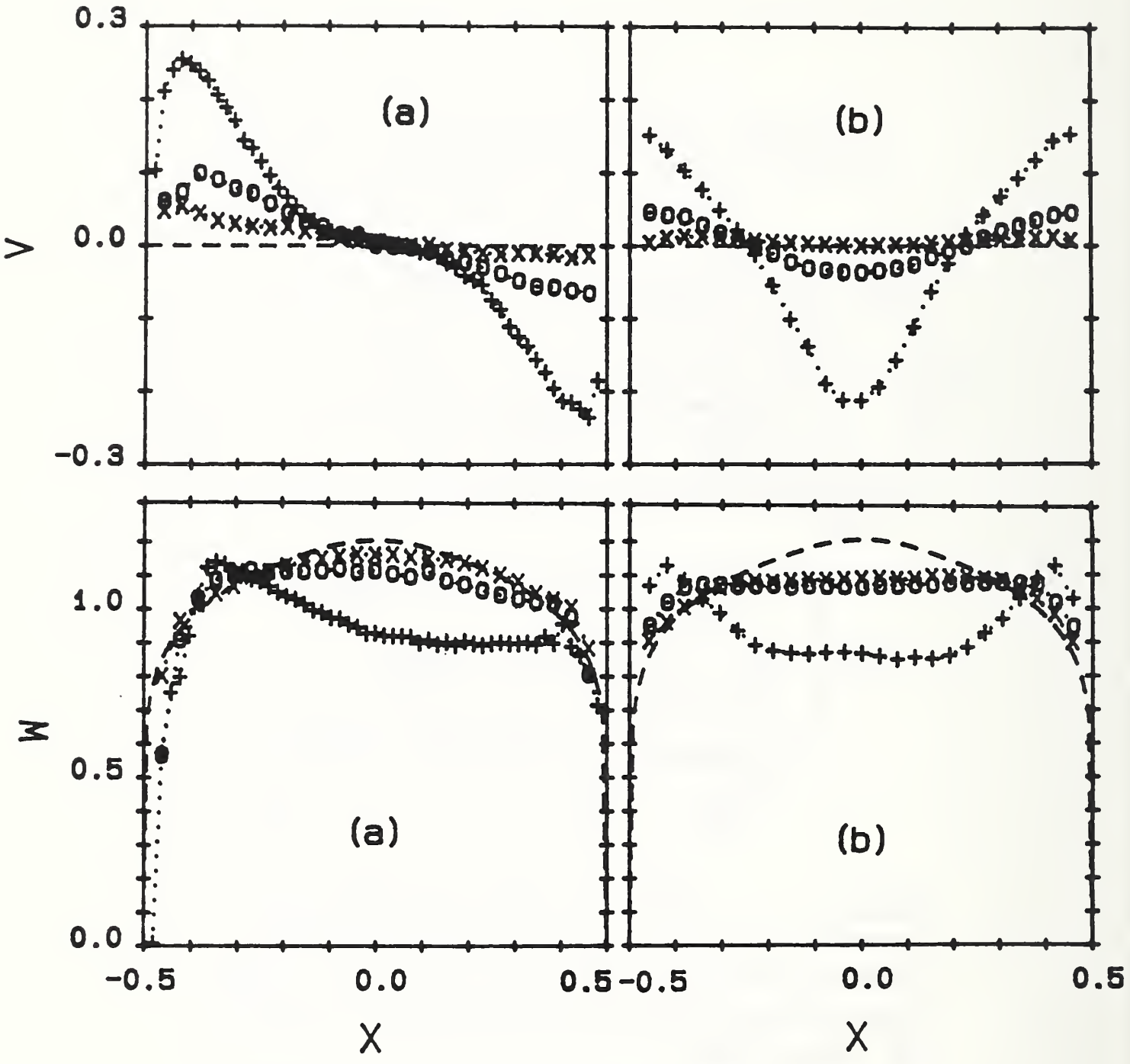

Figure 2 - Cross-stream Profiles of the Mean Vertical and Streamwise Velocity Components (a) Double-Elbows-Out-of-Plane, Closely Coupled (+, z = 2.6; 0, z = 31.8; and x, z = 91.3) (b) Single Elbow (+, z = 2.7; 0, z = 11.2; x, z = 23.2) Dotted Lines Refer to Ideal Pipeflow Profiles for Smooth Pipe and Reynolds Number = 10^5; Power Law Exponent, n = 7.0.

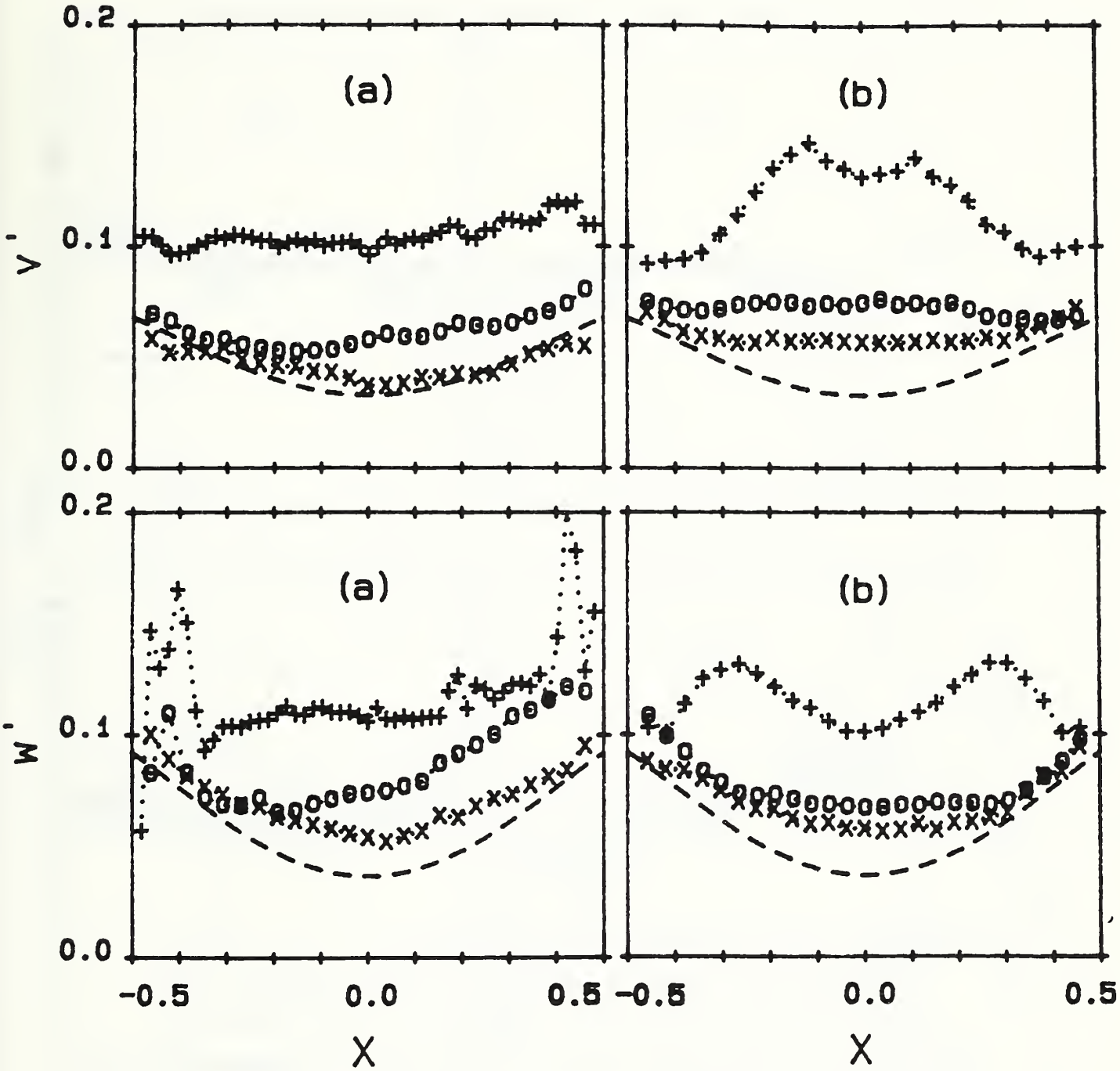

Figure 3 - Cross-stream Profiles of the Root-Mean-Square (r.m.s.) Components of the Vertical and Streamwise Components of the Turbulent Velocity at Successive Stream Stations:
(a) Double-Elbows Out-of-Plane, Closely Coupled, (+, z = 2.6; 0, z = 31.8; and x, z = 91.3) and
(b) Single Elbow (+, z = 2.7; 0, z = 11.2; x, z = 23.2)
Dotted Lines Refer to Laufer's Data.

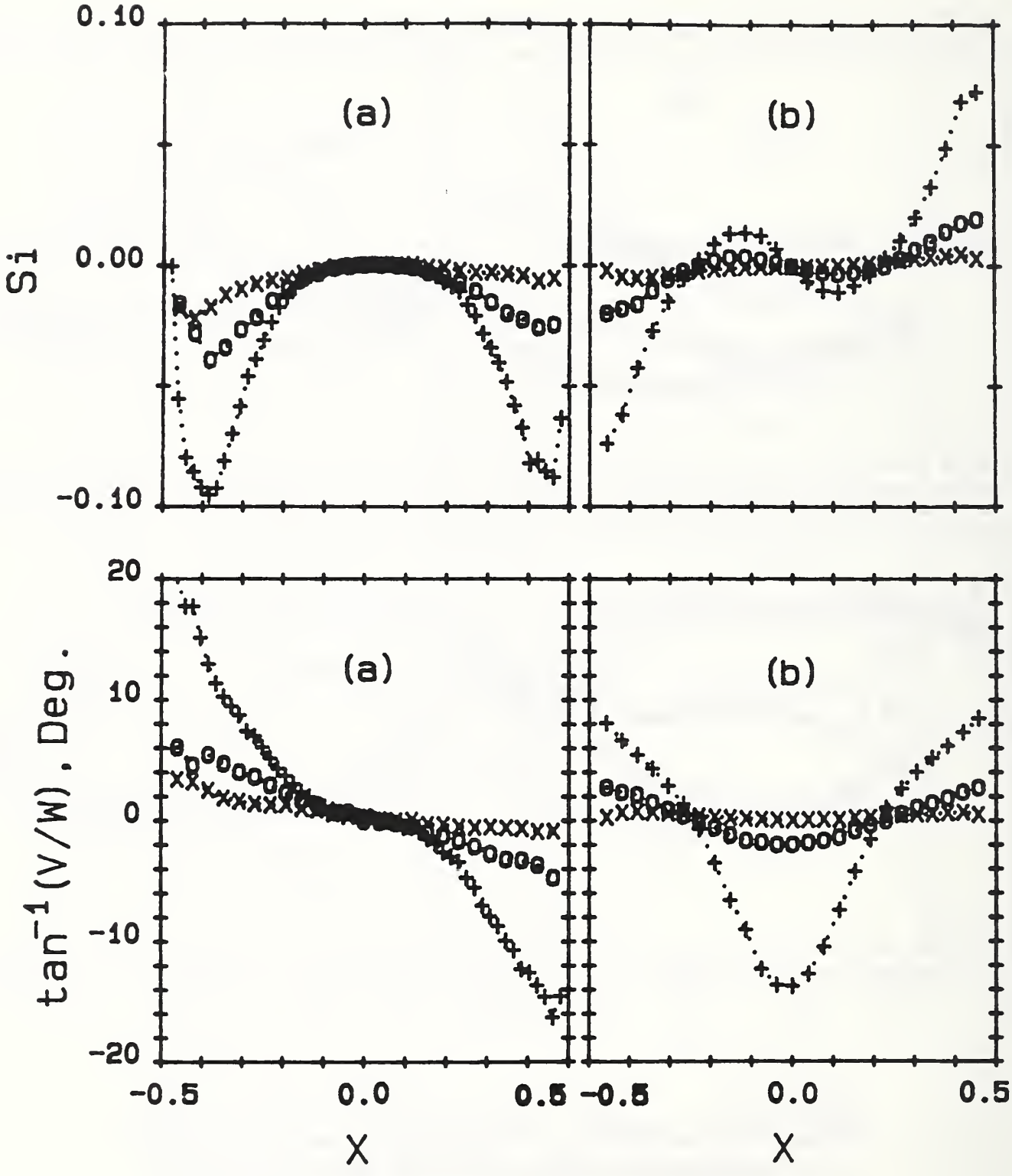

Figure 4 - Cross-stream Profiles of the Swirl Intensity, Si and the Swirl Angle ($\tan^{-1}$ V/W) at Successive Stream Stations: (a) Double-Elbows-Out-of-Plane, Closely Coupled, (+, z = 2.6; 0, z = 31.8; x, z = 91.2), and (b) Single Elbow, (+, z = 2.7; 0, z = 11.2; x, z = 23.2)

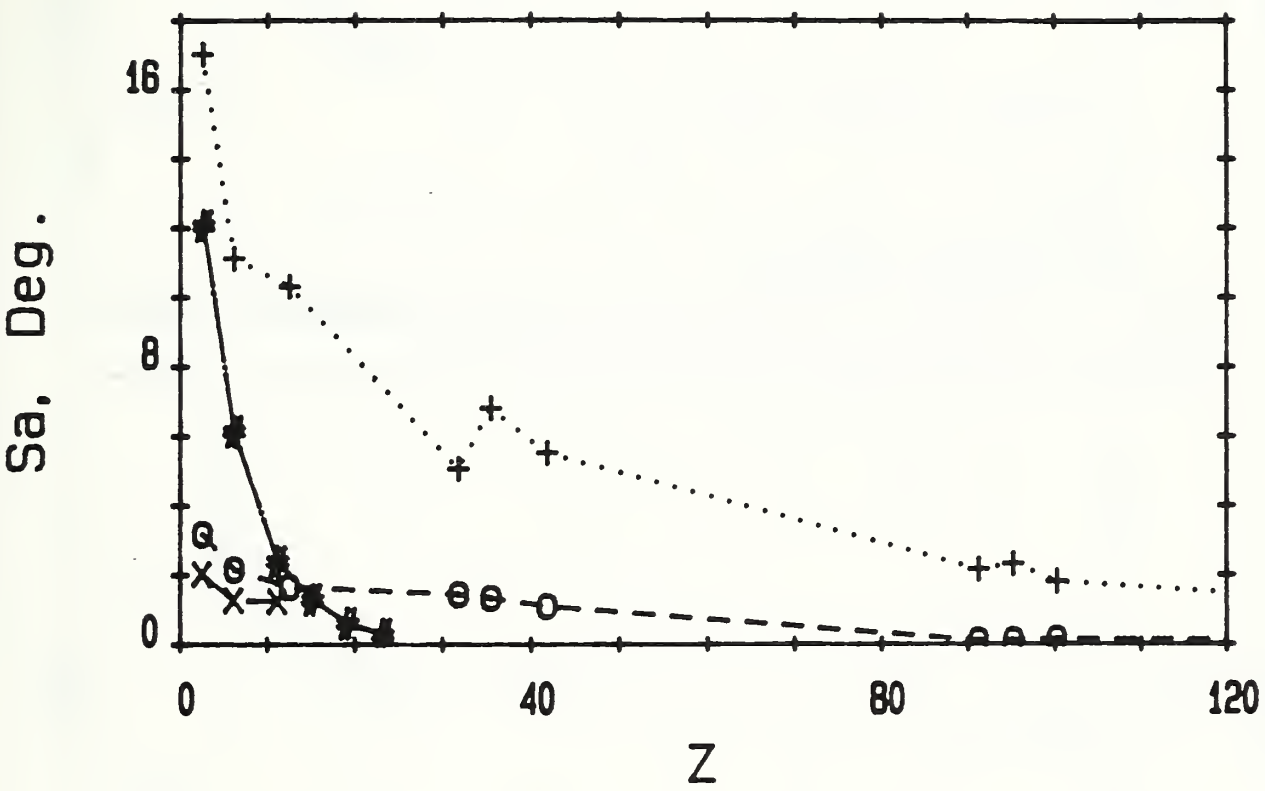

Figure 5 - Streamwise Distribution of Sa. Double Elbows-Out-of-Plane: Closely Spaced (+) Spaced 2.4 Diameters (0), Spaced 5.3 Diameters (x), and Single Elbow (#).

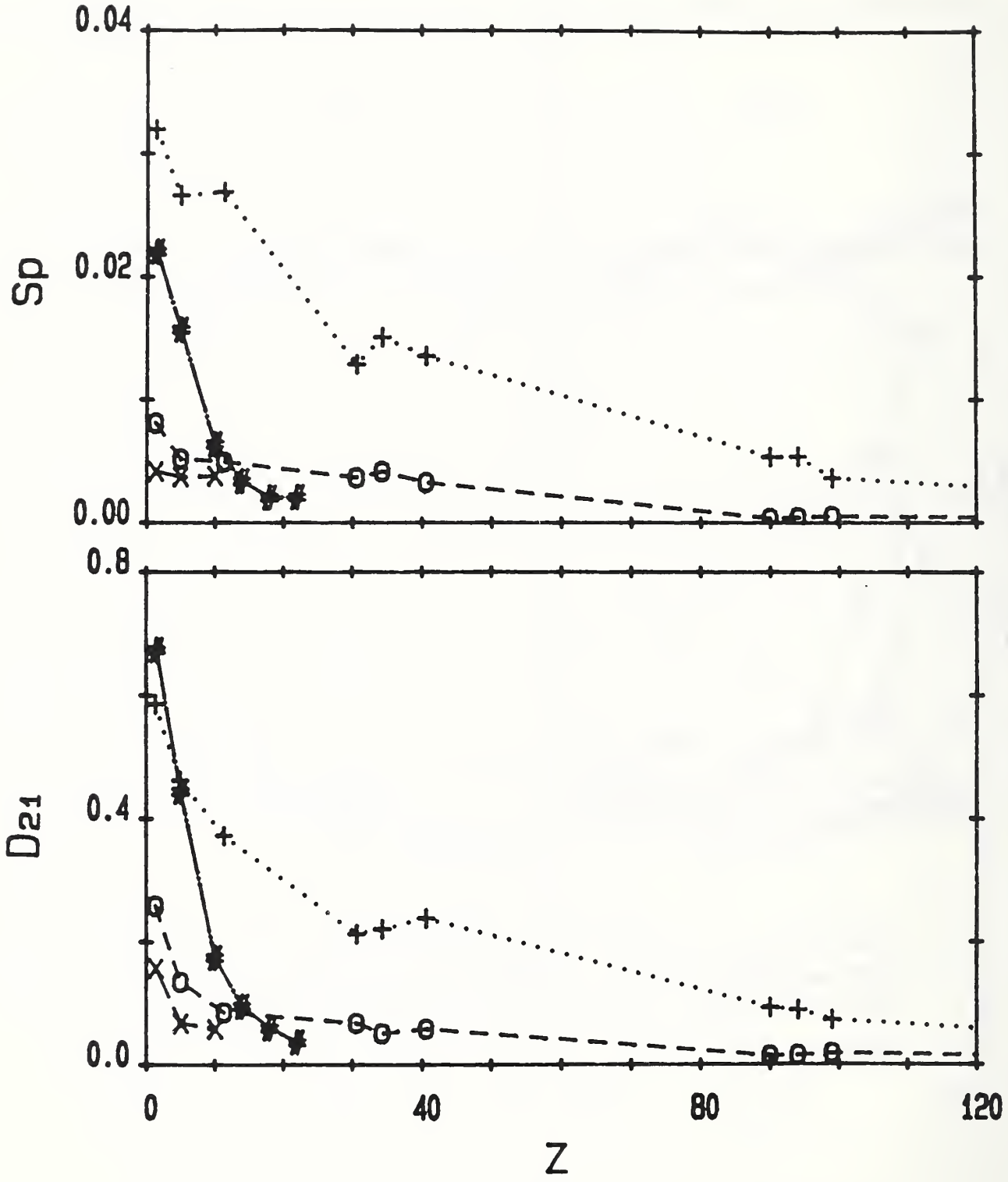

Figure 6 - Streamwise Distributions of the Parameters Sp and D_{21} for the Double Elbows-Out-of-Plane Configurations: (+, Closely Coupled; 0, Spaced 2.4 Diameters; x, Spaced 5.3 Diameters) and the Single Elbow (#)

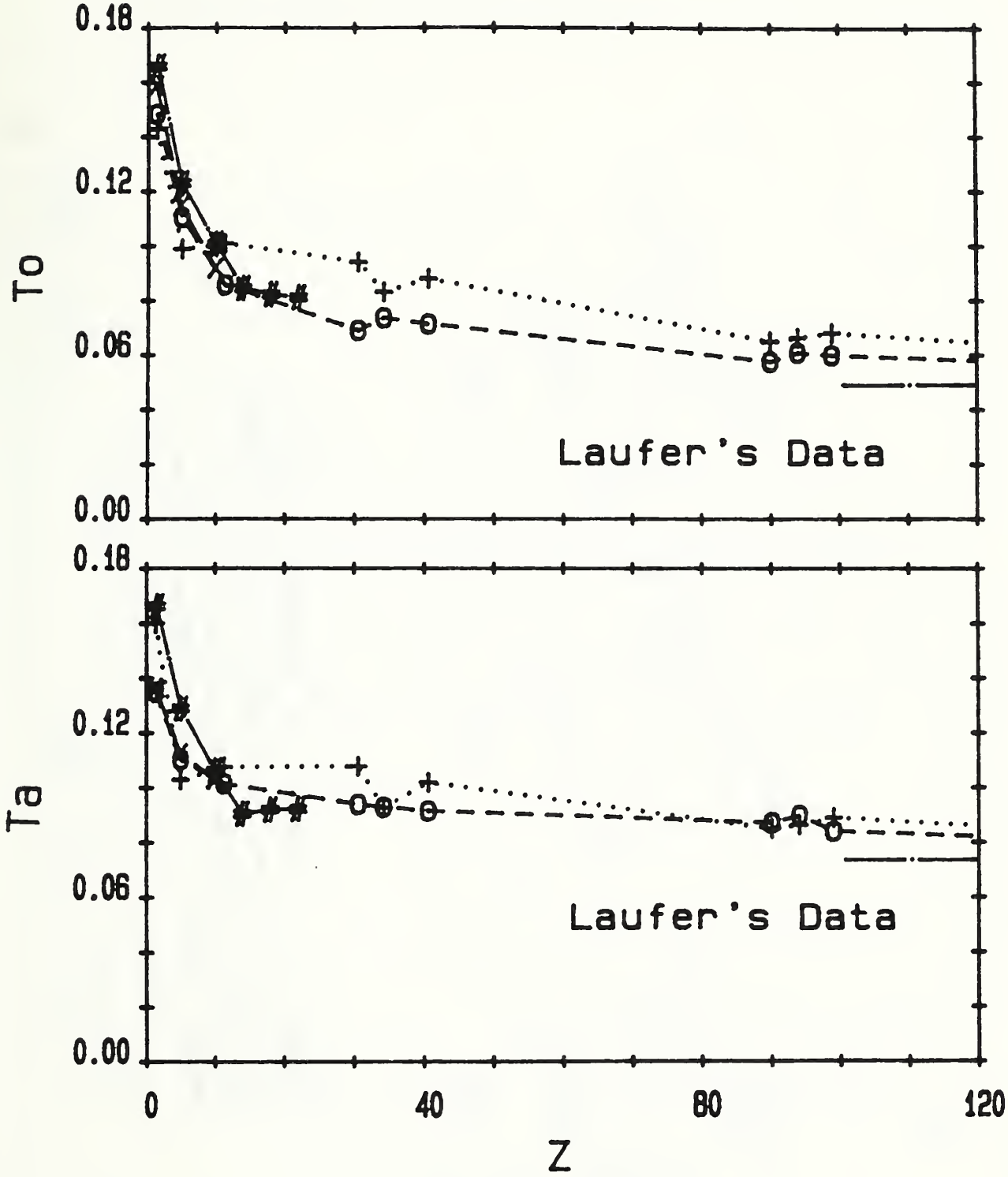

Figure 7 - Streamwise Distributions of Centerline Turbulence, To and Averaged Along Horizontal Diameters, Ta. Double Elbows-Out-of-Plane: Closely Spaced (+); Spaced 2.4 Diameters (0); Spaced 5.3 Diameters (x); and Single Elbow (#)

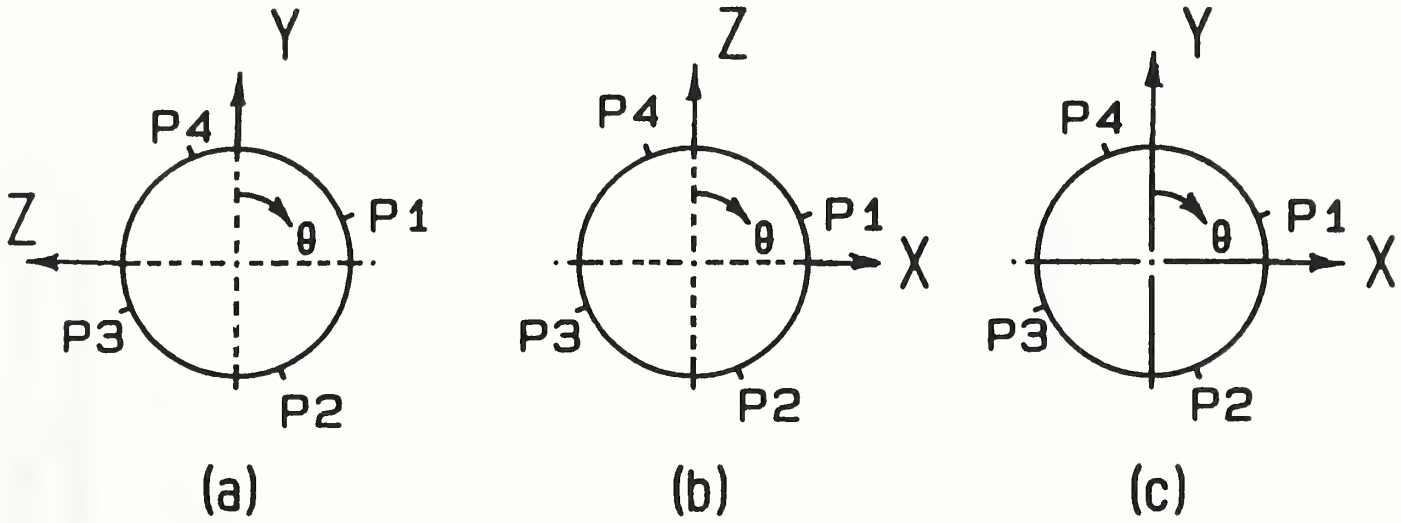

Figure 8 - Sketches of Azimuthal Locations (looking upstream) of Pressure Taps at Lettered Streamwise Stations: (a) Double Elbows-Out-of-Plane, Station A, (b) Single Elbow, Station A, and (c) All Downstream Stations B,C, and D. Angle Values are: $0_1 = 67.5$; $0_2 = 157.5$; $0_3 = 247.5$; $0_4 = 337.5$

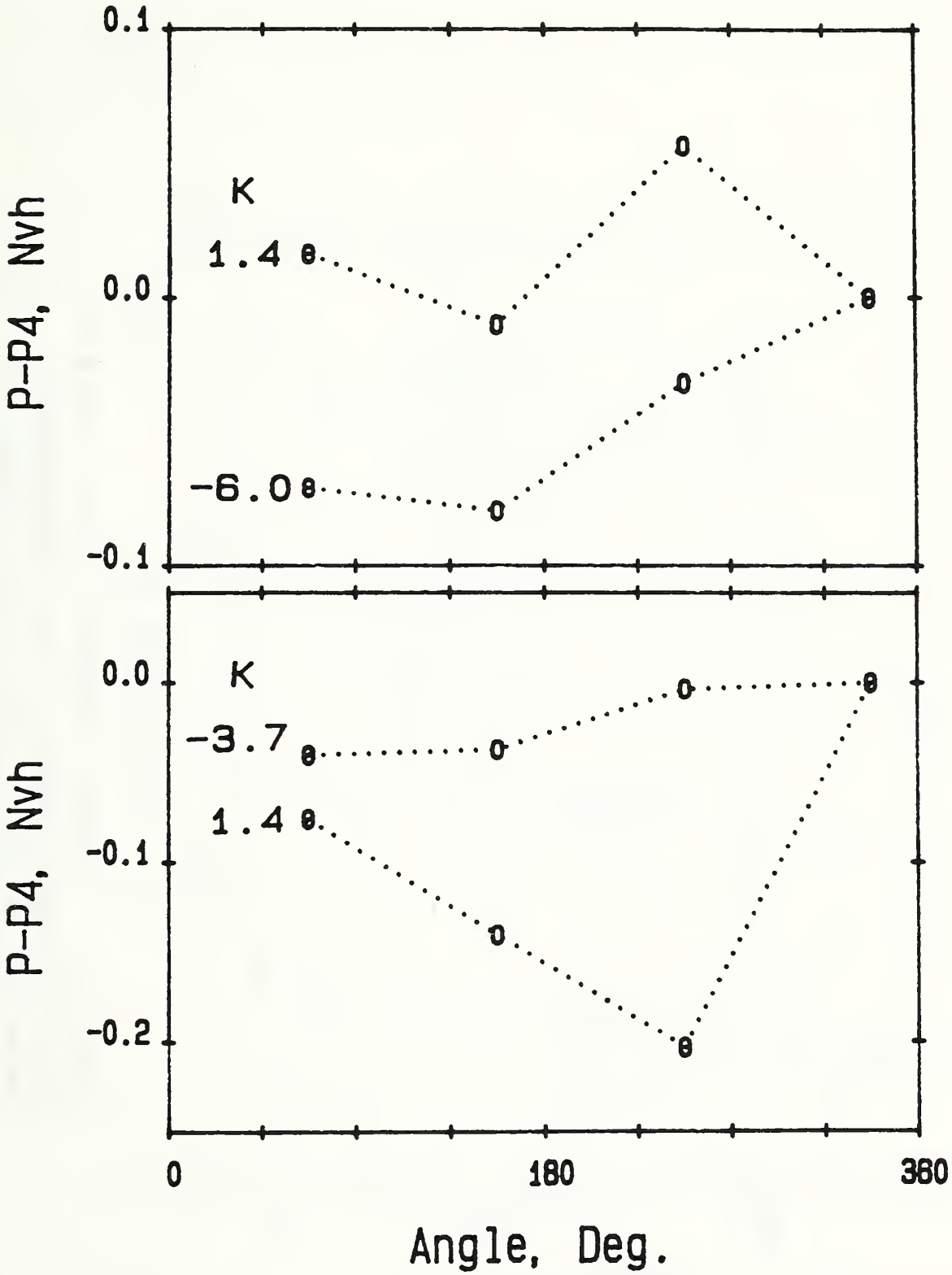

Figure 9 - Azimuthal Variations in static Pressure Relative to that measured at Tap No. 4 at Stream Stations Up and Downstream of the Elbow Configuration. Pressure Differences are Given in "Velocity Heads". Double Elbows-Out-of-Plane Results, (a); Single Elbow Results (b). Reynolds Number $= 10^5$.

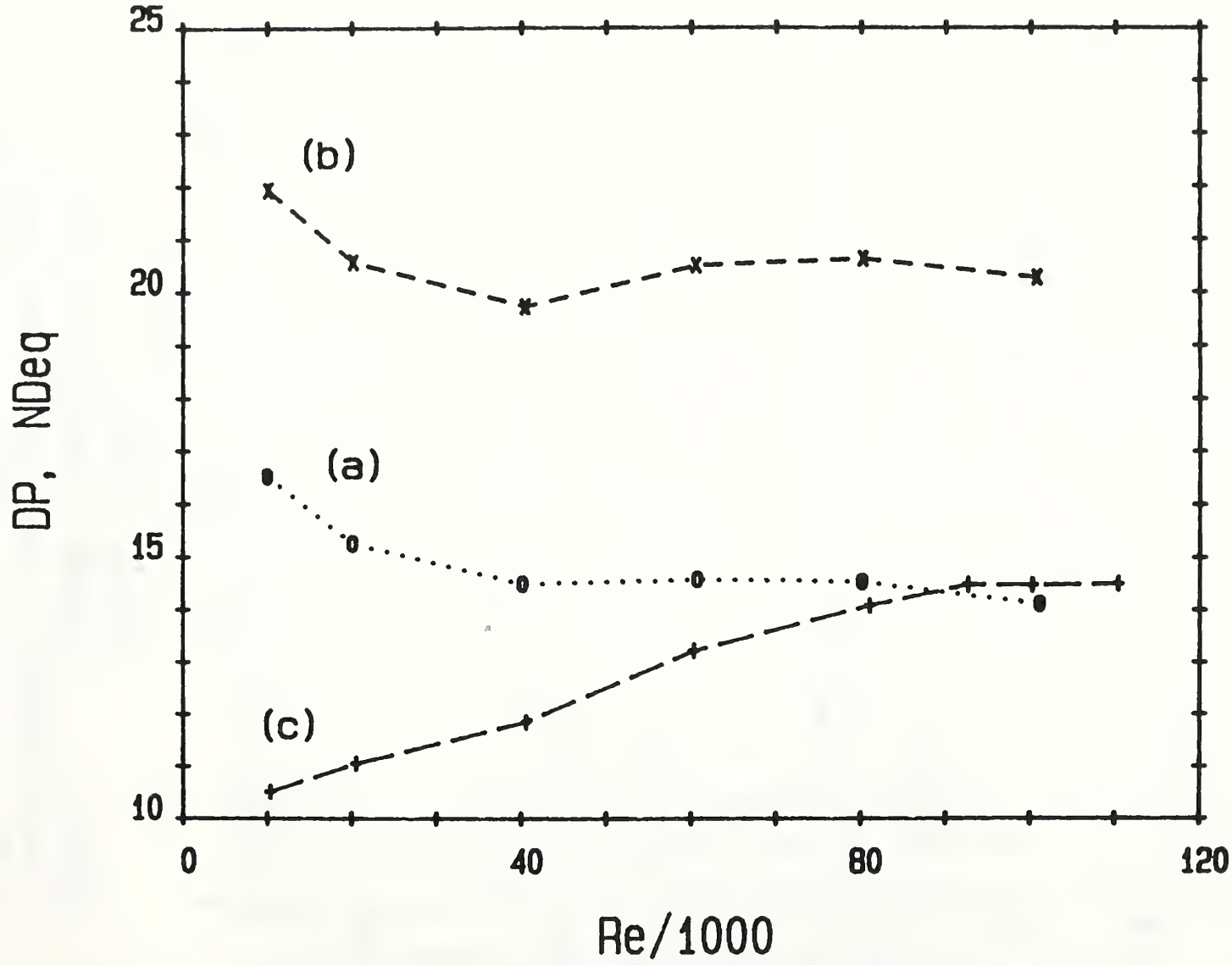

Figure 10 - Pressure Differences versus Reynolds Number Through Different Elbow Configurations. Double Elbows-Out-of-Plane: Closely Coupled (a), Spaced 2.4 Diameters (b), and Single Elbow (c).

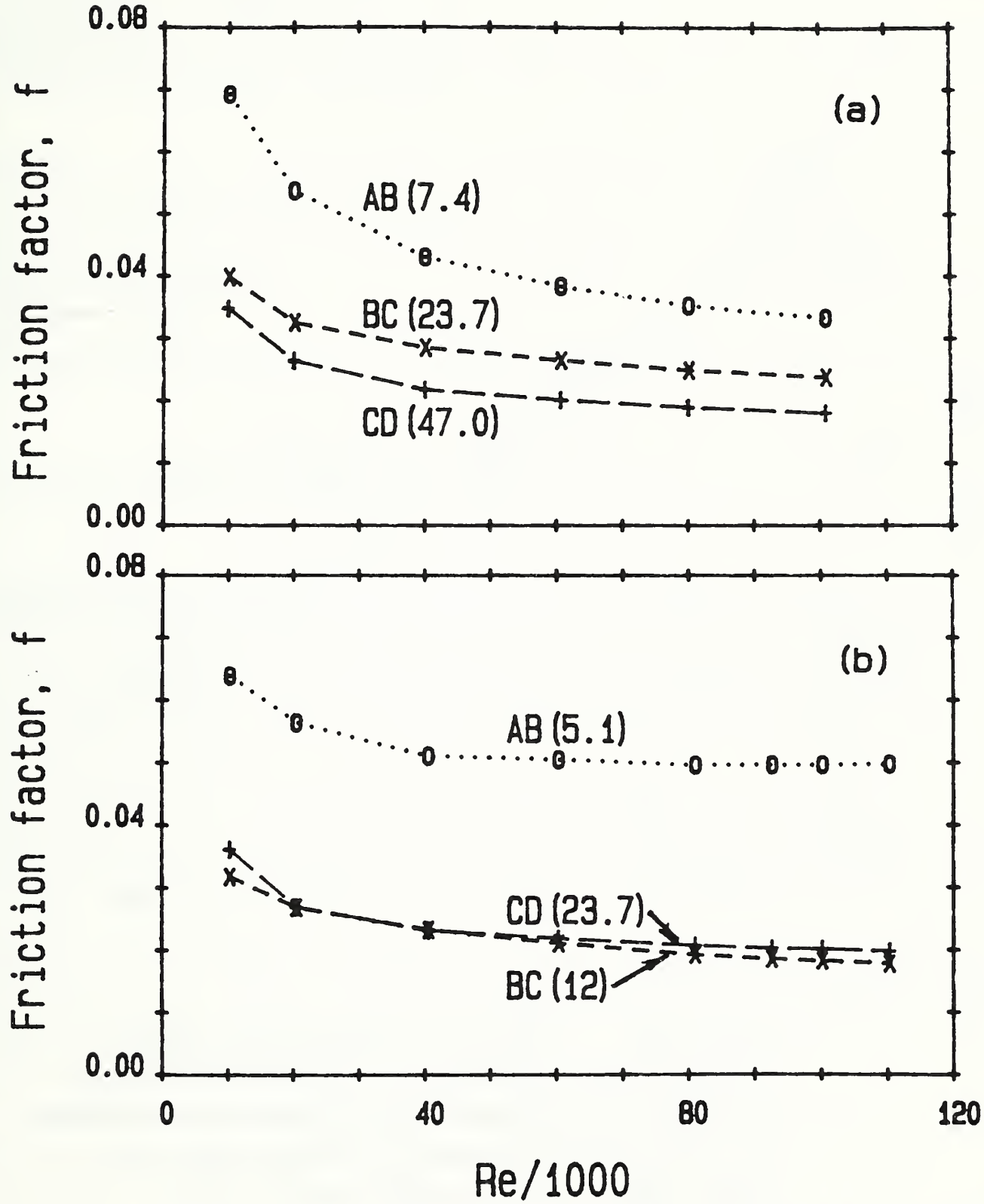

Figure 11 - Friction Factor versus Reynolds Number Through Different Piping Configurations. Double Elbows-Out-of-Plane, (a); Single Elbow, (b) Respective Station Separations are given in Parentheses.

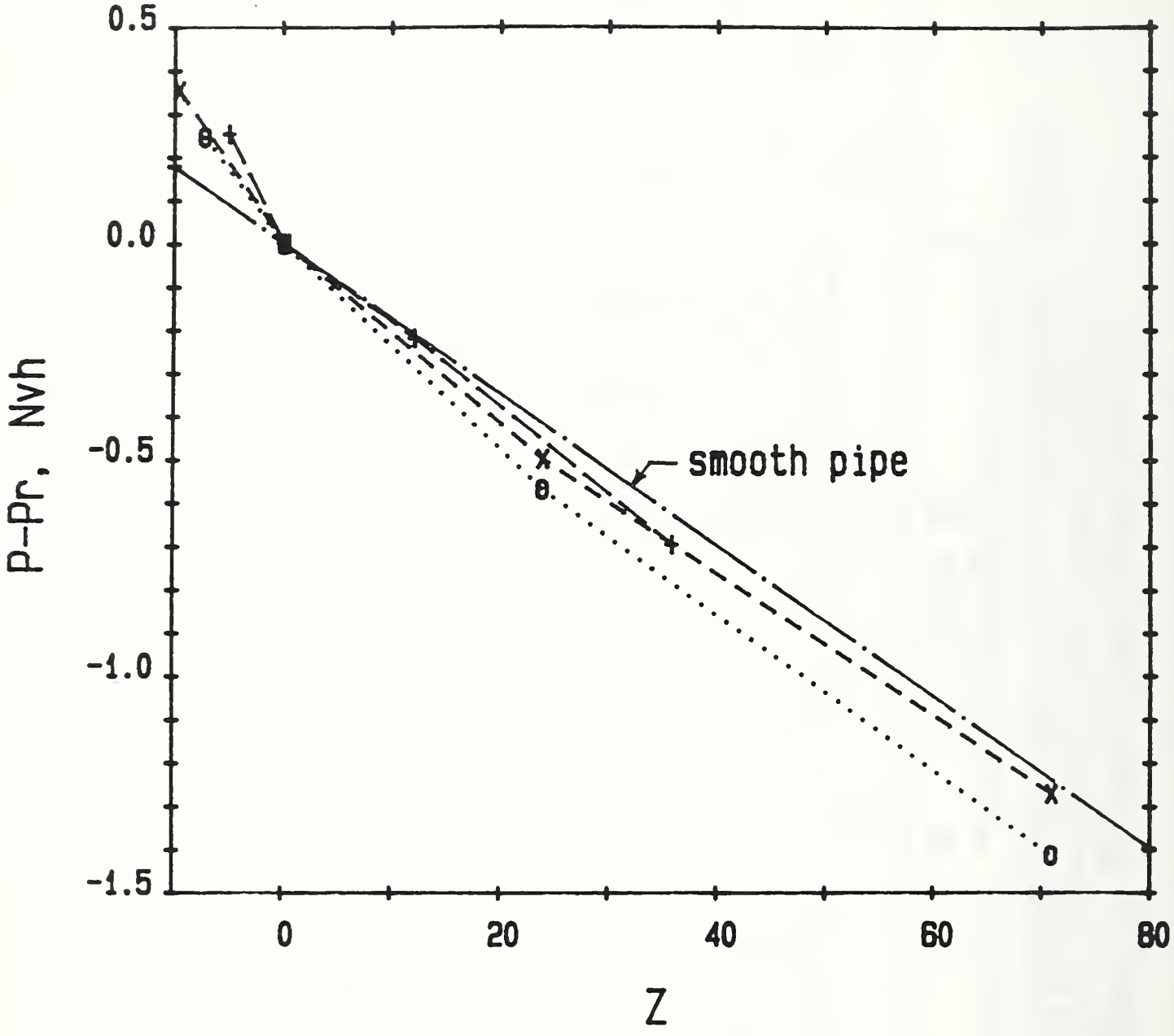

Figure 12 - Pressure Differences (in Velocity Heads) versus Streamwise Distance Compared to Smooth Pipe Results. Double Elbows-Out-of-Plane: Closely Spaced (0), Spaced 2.4 Diameters (x); Single Elbow (+). Reynolds Number = 10^6.

NBS-114A (REV. 2-8C)

U.S. DEPT. OF COMM. **BIBLIOGRAPHIC DATA SHEET** (See instructions)	1. PUBLICATION OR REPORT NO. NISTIR 89-4029	2. Performing Organ. Report No.	3. Publication Date JANUARY 1989

4. TITLE AND SUBTITLE

Mixing Motions Produced by Pipe Elbows

5. AUTHOR(S)

T.T. Yeh and G.E. Mattingly

6. PERFORMING ORGANIZATION (If joint or other than NBS, see instructions)

NATIONAL BUREAU OF STANDARDS
DEPARTMENT OF COMMERCE
WASHINGTON, D.C. 20234

7. Contract/Grant No.

8. Type of Report & Period Covered

9. SPONSORING ORGANIZATION NAME AND COMPLETE ADDRESS (Street, City, State, ZIP)

10. SUPPLEMENTARY NOTES

☐ Document describes a computer program; SF-185, FIPS Software Summary, is attached.

11. ABSTRACT (A 200-word or less factual summary of most significant information. If document includes a significant bibliography or literature survey, mention it here)

Mixing can be done using various techniques - stirred tanks, fluid injections schemes, or via a range of elements placed inside pipelines to produce mixedness through the generation of secondary flows and turbulence levels at the expense of fluid pipeline pressure. In this paper, elbow configurations are examined for their potential as effective pipeline mixers.

Experimental measurements have been made, using laser Doppler velocimetry (LDV) of the pipeflows produced by a range of pipe-elbow configurations. The secondary flow characteristics of these pipeflows are described qualitatively and quantitatively together with their decay rates in the downstream piping. The potential these flows have as mixing environments is described on the basis of the profiles of the mean and turbulent velocity components, the change of these with downstream distance, and the pressure losses.

Parameters characterizing these flow fields are defined from the measured velocity profiles. It is shown that double elbow "out-of-plane" combinations where minimal pipe-lengths separate the elbows can produce very energetic, long-lasting, swirling flows that can serve as effective mixers. Such effectiveness suggests that process designers might consider adding an additional elbow (and the slight increase in pressure loss) to pipe turns so as to take advantage of the enhanced mixedness that can be achieved via close-coupled elbows-out-of-plane.

12. KEY WORDS (Six to twelve entries; alphabetical order; capitalize only proper names; and separate key words by semicolons)

elbow; LDV measurements; Mixing; pipe flows ; turbulence; swirl; coherent structure; pressure losses; vorticity

13. AVAILABILITY

☒ Unlimited

☐ For Official Distribution. Do Not Release to NTIS

☐ Order From Superintendent of Documents, U.S. Government Printing Office, Washington, D.C. 20402.

☒ Order From National Technical Information Service (NTIS), Springfield, VA. 22161

14. NO. OF PRINTED PAGES

40

15. Price

$11.95

USCOMM-DC 6043-P80